

# Analysis of multicrystalline silicon solar cells by modified 3-diode equivalent circuit model taking leakage current through periphery into consideration

Kensuke Nishioka<sup>a,\*</sup>, Nobuhiro Sakitani<sup>b</sup>, Yukiharu Uraoka<sup>b</sup>, Takashi Fuyuki<sup>b</sup>

<sup>a</sup>Graduate School of Materials Science, Japan Advanced Institute of Science and Technology, 1-1 Asahidai, Nomi, Ishikawa, 923-1292, Japan

<sup>b</sup>Graduate School of Materials Science, Nara Institute of Science and Technology, 8916-5 Takayama, Ikoma, Nara 630-0101, Japan

Received 2 April 2007; accepted 3 April 2007

Available online 7 May 2007

## Abstract

We proposed a modified 3-diode equivalent circuit model for analysis of multicrystalline silicon (Mc-Si) solar cells. By using this equivalent circuit model, we can precisely evaluate the characteristics of Mc-Si solar cells taking the influence of grain boundaries and large leakage current through the peripheries into consideration and extract electrical properties. The calculated value of current-voltage characteristics for small size (3 mm × 3 mm) Mc-Si solar cells using this model completely agreed with the measured value at various cell temperatures. Moreover, the calculated open-circuit voltage ( $V_{oc}$ ) obtained by extracted parameters and measured  $V_{oc}$  agreed well.

© 2007 Elsevier B.V. All rights reserved.

**Keywords:** Solar cell; Equivalent circuit; Multicrystalline silicon; Leakage current; Temperature

## 1. Introduction

Photovoltaic power generation is becoming increasingly widespread as a clean energy source that is gentle to the earth. Especially, multicrystalline silicon (Mc-Si) is increasingly applied for the fabrication of photovoltaic devices as a low-cost material. In order to comprehend the output performance of Mc-Si solar cells, it is important to analyze their electrical properties.

Ordinarily, the electrical properties of solar cells have been analyzed using a simple equivalent circuit [1–4]. However, the electrical properties of Mc-Si solar cells depend on many factors such as grain boundaries, and it is difficult to analyze the properties by a simple equivalent circuit [5]. Moreover, when we deal with small size solar cells which are in development phase, it is difficult to perform precise analysis due to comparatively large leakage current through peripheries of solar cells.

In this paper, a modified 3-diode equivalent circuit model for Mc-Si solar cells with large leakage current is

proposed. By using this equivalent circuit model, we can take the influence of grain boundaries and leakage current through the peripheries into consideration and extract electrical properties of Mc-Si solar cells.

## 2. Current–voltage measurement of solar cells

We measured current-voltage ( $I$ – $V$ ) curves of small size (3 mm × 3 mm) samples of Mc-Si solar cells (Mc-Si-A, B, and C) under conditions of darkness and illumination (AM1.5G). Each cell has a conventional  $n^+/p/p^+$  structure, silicon nitride passivation coating, and 300  $\mu\text{m}$  thickness. The  $n^+$  and  $p^+$  layers were fabricated by the diffusion of the phosphorous and aluminum on boron-doped p-type cast Si. The resistivity of p-type Si was 1  $\Omega\text{cm}$ .

Analysis of the temperature characteristics is necessary, because temperature is an important parameter that governs semiconductor carrier transport. Then,  $I$ – $V$  measurement was carried out at temperature from 20 to 100 °C in steps of 20 °C.

The photovoltaic characteristics of cells (short-circuit current density ( $J_{sc}$ ), open-circuit voltage ( $V_{oc}$ ), fill factor

\*Corresponding author. Tel.: +81 761 51 1562; fax: +81 761 51 1149.

E-mail address: [nishioka@jaist.ac.jp](mailto:nishioka@jaist.ac.jp) (K. Nishioka).

(FF) and conversion efficiency ( $\eta$ ) measured at 20 °C are shown in Table 1.

### 3. Extraction of electrical properties by modified multi-diode equivalent circuit model

Fig. 1(a) shows a conventional single-diode model representing a solar cell, and characterizes the typical electrical properties of solar cells [3].  $R_s$  and  $R_{sh}$  express series resistance and shunt resistance, respectively. It is reported that we cannot calculate the  $I$ – $V$  characteristics of solar cells precisely by using a conventional single-diode model [5].

Fig. 1(b) shows the modified 2-diode model that we have proposed [6]. Diodes  $D_1$  with  $n = 1$  and  $D_2$  with  $n = 2$  are connected in parallel. This model can separate the diffusion current component ( $n = 1$ ) and recombination current component ( $n = 2$ ), and the effects of recombination are mainly expressed by  $D_2$ . In the vicinity of grain boundaries, recombination of minority carriers easily occurs.  $r$  is defined as the ratio of the recombination area, in which the recombination of minority carriers is pronounced. In this model,  $R_s$  is divided into three components of  $R_{s1}$  connected to  $D_1$ ,  $R_{s2}$  connected to  $D_2$  and  $R_{sub}$  that

expresses other resistances owing to such as the substrate, and microscopic inhomogeneity of resistivity at the recombination sites can be considered separately.

In the equivalent circuit of the modified 2-diode model, the saturation current density for  $D_1$  ( $J_{01}$ ) is defined as

$$J_{01} = q\sqrt{(D_n/\tau_n)} \cdot (n_i^2/N_A), \quad (1)$$

where  $q$ ,  $D_n$ ,  $\tau_n$ ,  $n_i$ , and  $N_A$  are the electron charge, diffusion coefficient for electrons, lifetime of minority carriers, intrinsic carrier density and acceptor density, respectively.

The saturation current density for  $D_2$  ( $J_{02}$ ) is defined as

$$J_{02} = (qWn_i/2) \cdot \sigma v_{th} N_t = qWn_i/2\tau_r, \quad (2)$$

where  $W$ ,  $\sigma$ ,  $v_{th}$ ,  $N_t$  and  $\tau_r$  are the depletion layer width, cross section, thermal velocity of electrons, density of recombination centers and effective lifetime of minority carriers, respectively. The total current density  $J$  is obtained as

$$J = J_1 + J_2 + J_{sh} \quad (3)$$

$$J_{sh} = V/R_{sh} \quad (4)$$

$$V_{D1} = V - J_1 R_{s1} - (J_1 + J_2) R_{sub} \quad (5)$$

$$V_{D2} = V - J_2 R_{s2} - (J_1 + J_2) R_{sub} \quad (6)$$

$$J_1 = (1 - r) \cdot J_{01} \{\exp(qV_{D1}/kT) - 1\} \quad (7)$$

$$J_2 = r \cdot J_{02} \{\exp(qV_{D2}/2kT) - 1\}, \quad (8)$$

where  $V_{D1}$  and  $V_{D2}$  are the voltages applied to  $D_1$  and  $D_2$ , and  $J_1$ ,  $J_2$  and  $J_{sh}$  are the current densities through  $D_1$ ,  $D_2$  and  $R_{sh}$ , respectively and  $T$  is the absolute temperature. By

Table 1  
Photovoltaic characteristics for all cells at 20 °C (100 mW cm<sup>2</sup>, AM1.5G)

	$V_{oc}$ (V)	$J_{sc}$ (mA/cm <sup>2</sup> )	FF	$\eta$ (%)
Mc-Si-A	0.574	30.37	0.644	11.23
Mc-Si-B	0.579	33.03	0.661	12.64
Mc-Si-C	0.568	29.57	0.715	12.01

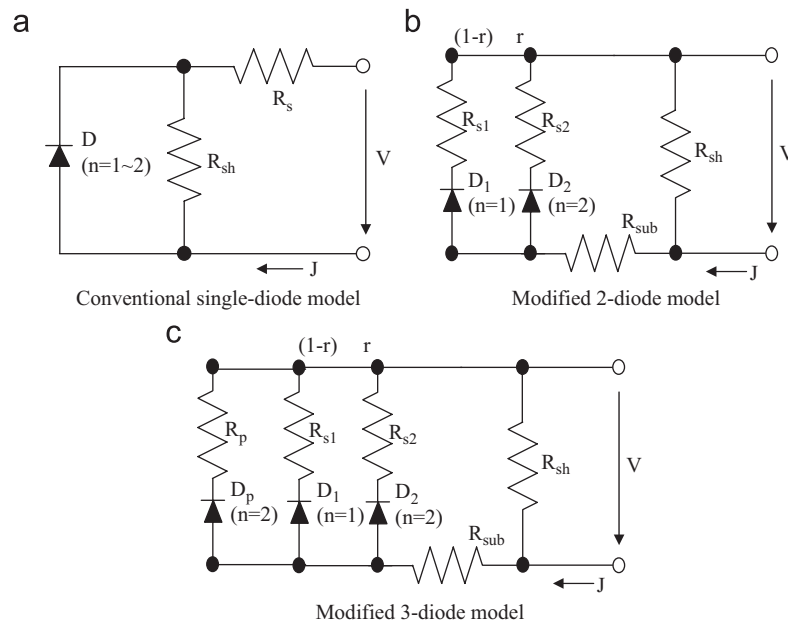


Fig. 1. Schematics of equivalent circuits for solar cells without current sources, (a) conventional single-diode model, (b) modified 2-diode model, and (c) modified 3-diode model.

using modified 2-diode equivalent circuit model, we can calculate solar cell's characteristics considering diffusion and recombination currents separately. It has been reported that the calculated values of  $I$ – $V$  characteristics using the modified 2-diode model fitting agreed completely with the measured values, and the validity of fitting parameters was verified [6].

We can perform precise fitting of  $I$ – $V$  curves by using modified 2-diode model. However, if we deal with small size solar cells, it is difficult to perform precise fitting because the leakage current through peripheries considerably affect the  $I$ – $V$  characteristics of solar cells. So, in this study, we proposed the modified 3-diode model that was able to take the leakage current through the periphery into consideration. In the precise fitting using equivalent circuit, we cannot express large leakage current through periphery by only  $R_{sh}$ . It is considered that the recombination of minority carriers is enhanced at the surface of peripheries. Then, a diode  $D_p$  with  $n = 2$  that was able to express the leakage current through the peripheries was added to the modified 2-diode model. Fig. 1(c) shows the modified 3-diode model. For the modified 3-diode model, eight variable parameters,  $J_{01}$ ,  $J_{02}$ ,  $J_{0p}$ ,  $r$ ,  $R_{s1}$ ,  $R_{s2}$ ,  $R_{sh}$  and  $R_p$  were considered.  $R_{sub}$  was treated as a fixed parameter. In solar cells of  $1\ \Omega\text{cm}$  resistivity and  $300\ \mu\text{m}$  thickness, the specific resistance of the p-type substrate  $R_{sub}$  can be estimated as approximately  $0.03\ \Omega\text{cm}^2$ .

As shown in Fig. 1(c), the modified 3-diode model has two diodes with  $n = 2$  ( $D_2$  and  $D_p$ ). It is therefore extremely important to distinguish the current component of  $D_2$  ( $J_2$ ) from that of  $D_p$  ( $J_p$ ). It is considered that the leakage current  $J_p$  has an effect on the low bias region in  $I$ – $V$  curve;

on the contrary,  $J_2$  has an effect on the higher bias region. Then,  $J_2$  and  $J_p$  were distinguished by setting as  $R_p \gg R_2$ . The fitting parameters in the modified 3-diode model were varied so that the calculated values obtained by these equations should agree with the measured values.

## 4. Results and discussion

### 4.1. Comparison of measured and calculated values

Figs. 2(a) and 2(b) show the measured and calculated values of the current density–voltage ( $J$ – $V$ ) curve for the Mc-Si-A under the dark condition at  $20^\circ\text{C}$ . The calculated value was obtained by the modified 3-diode model. The calculated value completely agreed with the measured value in the voltage region of  $0$ – $1.0\ \text{V}$ . Moreover, it is possible to separate the current into the diffusion current component ( $J_1$ ), recombination current component ( $J_2$ ), shunt current component ( $J_{sh}$ ), and leakage current component ( $J_p$ ) by this calculation method. Table 2 shows the electrical properties of all three Mc-Si solar cells (Mc-Si-A, B and C) obtained from  $J$ – $V$  curve fitting by modified 3-diode model.

Figs. 3(a) and 3(b) show the measured and calculated values of the  $J$ – $V$  curve for the Mc-Si-A under the dark condition at  $100^\circ\text{C}$ . The calculated value was obtained by the modified 3-diode model. The calculated value agreed well with the measured value. The modified 3-diode model was applicable for  $J$ – $V$  curve fitting of small size solar cells at various cell temperatures. Table 2 also shows the electrical properties of Mc-Si-A at  $100^\circ\text{C}$ .

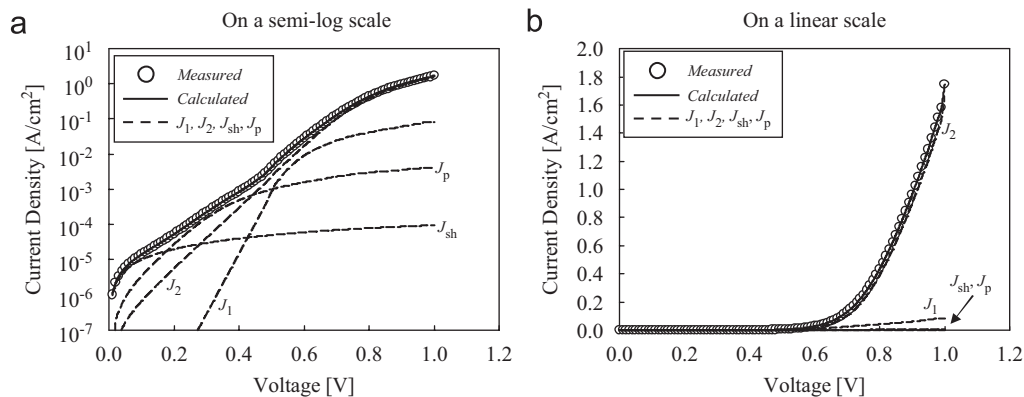


Fig. 2. Fitting results of the forward  $J$ – $V$  curve for Mc-Si-A at  $20^\circ\text{C}$ , (a) on a semi-log scale and (b) on a linear scale.

Table 2  
Electrical properties of solar cells obtained by fitting

	$J_{01}$ (A/cm <sup>2</sup> )	$J_{02}$ (A/cm <sup>2</sup> )	$J_{0p}$ (A/cm <sup>2</sup> )	$r$	$R_{s1}$ ( $\Omega\text{cm}^2$ )	$R_{s2}$ ( $\Omega\text{cm}^2$ )	$R_{sh}$ ( $\Omega\text{cm}^2$ )	$R_p$ ( $\Omega\text{cm}^2$ )
Mc-Si-A ( $20^\circ\text{C}$ )	$4.40 \times 10^{-12}$	$4.22 \times 10^{-7}$	$7.00 \times 10^{-7}$	0.32	5.0	0.08	10,000	130
Mc-Si-A ( $100^\circ\text{C}$ )	$3.02 \times 10^{-8}$	$9.76 \times 10^{-5}$	$1.50 \times 10^{-5}$	0.18	5.0	0.08	900	40
Mc-Si-B ( $20^\circ\text{C}$ )	$3.89 \times 10^{-12}$	$2.97 \times 10^{-7}$	$4.50 \times 10^{-7}$	0.42	5.0	0.27	20,000	200
Mc-Si-C ( $20^\circ\text{C}$ )	$5.33 \times 10^{-12}$	$4.34 \times 10^{-7}$	$1.10 \times 10^{-6}$	0.39	5.0	0.21	20,000	470

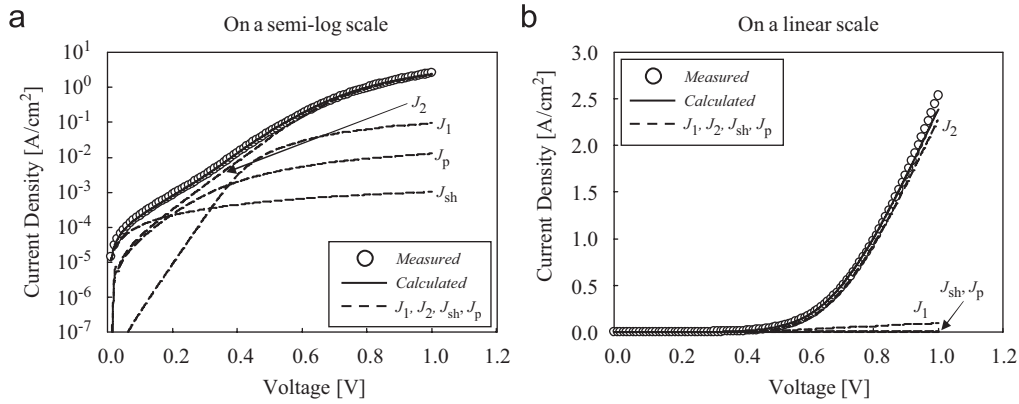


Fig. 3. Fitting results of the forward  $J$ - $V$  curve for Mc-Si-A at 100 °C, (a) on a semi-log scale and (b) on a linear scale.

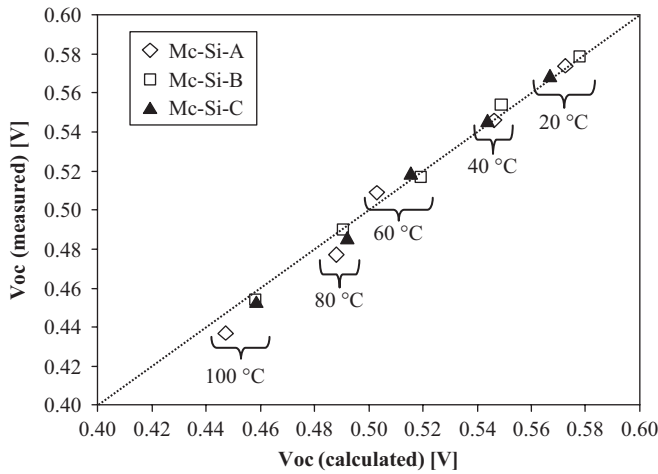


Fig. 4. Correlation between the  $V_{oc}$  calculated from  $J_{01}$  obtained by modified 3-diode model and the measured  $V_{oc}$ .

#### 4.2. Verification of fitting parameter obtained by modified 3-diode model (correlation between $J_{01}$ and $V_{oc}$ )

The current-voltage characteristic of ideal solar cells is given by

$$J = J_0 \left\{ \exp\left(\frac{qV}{nkT}\right) - 1 \right\} - J_{sc}, \quad (9)$$

where  $J_0$  is the saturation current density.

From Eq. (9),  $V_{oc}$  ( $J = 0$ ) is given by

$$V_{oc} = \frac{nkT}{q} \ln\left(\frac{J_{sc}}{J_0} + 1\right), \quad (10)$$

The  $J_{01}$  value obtained by fitting was substituted for  $J_0$  in Eq. (10), and the  $V_{oc}$  value was calculated.

Fig. 4 shows the correlation between  $V_{oc}$  calculated from  $J_{01}$  and the measured  $V_{oc}$  (AM1.5G, 100 mW/cm²). The correlations between calculated  $V_{oc}$  and measured  $V_{oc}$  at various cell temperatures are shown. The dashed line shows  $V_{oc}$  (measured) =  $V_{oc}$  (calculated from  $J_{01}$ ). The calculated  $V_{oc}$  obtained by the fitting parameter  $J_{01}$  and measured  $V_{oc}$  agreed well at all cell temperatures. These results demon-

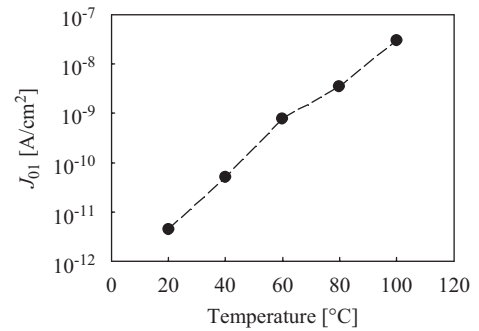


Fig. 5. Temperature dependence of saturation current density  $J_{01}$ .

strated that the values extracted by the fitting are reliable, and the modified 3-diode model was applicable for evaluation at various cell temperatures.

#### 4.3. Temperature characteristics of electrical properties obtained by modified 3-diode model

Fig. 5 shows the temperature dependence of  $J_{01}$  for the Mc-Si-A.  $J_{01}$  increased with increasing temperature.  $J_{01}$  and  $n_i$  are given by

$$J_{01} \propto n_i^2 \quad (11)$$

$$n_i = \sqrt{N_c N_v} \exp(-E_g/2kT), \quad (12)$$

where  $n_i$ ,  $N_c$ ,  $N_v$ , and  $E_g$  are the intrinsic carrier density, effective density of states in the conduction band, effective density of states in the valence band and energy band gap, respectively. As shown in Eqs. (11) and (12),  $J_{01}$  increases with increasing temperature. From Eq. (12), we can speculate that  $n_i^2$  increases in the 4th power with increasing temperature from 20 °C to 100 °C [7]. The increase in  $J_{01}$  with increasing temperature obtained by fitting using the modified 3-diode model agreed well with the calculated result by Eq. (12). Moreover, the validity of  $J_{01}$  has been explained in § 4.2. Thus, it is clarified that  $J_{01}$  obtained by fitting is useful for the analysis of cell performance.

Fig. 6 shows the temperature dependence of  $J_{02}$  for the Mc-Si-A.  $J_{02}$  increased with increasing temperature. It is considered that the value of  $J_{02}$  represents the quality of the

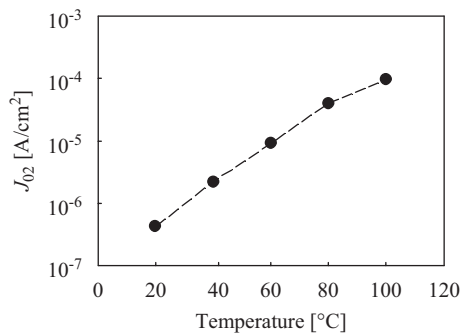


Fig. 6. Temperature dependence of saturation current due to recombination current density  $J_{02}$ .

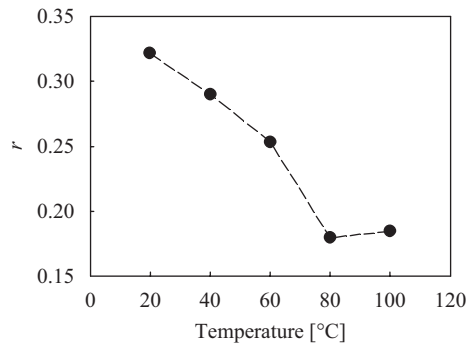


Fig. 7. Temperature dependence of ratio of recombination area  $r$ .

recombination center, and small  $J_{02}$  will lead to superior cell performance [5].

Fig. 7 shows the temperature dependence of  $r$  for the Mc-Si-A. It was found that  $r$  decreased with increasing temperature.  $r$  is defined as the ratio of the recombination area in which the recombination of minority carriers is pronounced. The recombination current component ( $n = 2$ ) is more dominant than the diffusion current component ( $n = 1$ ), when the value of  $r$  is large. The equilibrium of capture and emission processes determines the recombination fraction of minority carriers at the recombination centers. The emission probability increases when the temperature rises. Then, the number of free carriers that are not trapped at the recombination centers increases [8]. Therefore, the recombination fraction at the recombination centers decreases with increasing temperature, and the value of  $r$  decreases. Based on  $J$ - $V$  curve measurements and fitting by the modified 3-diode model, we can quantitatively evaluate the influence of recombination centers such as grain boundaries on the performance of solar cells. It has been reported that the typical value of  $r$  for single crystalline Si solar cell was 0.15 at 20 °C [6]. The values of  $r$  for the Mc-Si solar cells (Mc-Si-A: 0.32, Mc-Si-B: 0.42, Mc-Si-C: 0.39) at 20 °C are much larger than that for single crystalline Si. Compared with single crystalline Si, there are more recombination centers in Mc-Si such as grain boundaries and dislocations. Therefore, recombination of minority carriers occurred more frequently in Mc-Si solar cells, and the value of  $r$  became large.

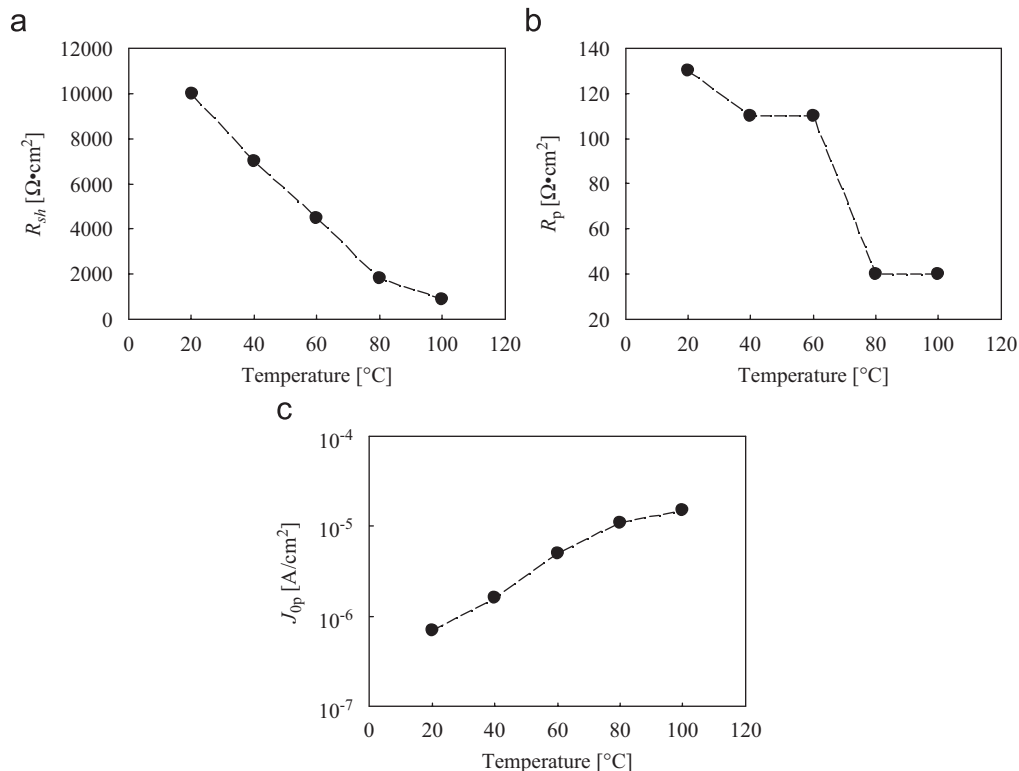


Fig. 8. Temperature dependence of (a)  $R_{sh}$ , (b)  $R_p$ , and (c)  $J_{0p}$ .

Fig. 8 show the temperature dependences of  $R_{sh}$ ,  $R_p$  and  $J_{0p}$  for the Mc-Si-A, respectively.  $R_{sh}$  and  $R_p$  decreased, and  $J_{0p}$  increased with increasing temperature. These results mean that the leakage current increases with increasing temperature. This is because the leakage current due to the carriers with large thermal velocity becomes dominant in the high-temperature range.

## 5. Conclusions

We proposed a modified 3-diode equivalent circuit model for analysis of Mc-Si solar cells with large leakage current through the periphery. By using this model, we can precisely evaluate the characteristics of Mc-Si solar cells taking the influence of grain boundaries and large leakage current through the periphery into consideration and extract electrical properties.

The calculated result by the modified 3-diode model agreed well with the measured  $J$ – $V$  curve. It was possible to separate the current into the diffusion current component ( $J_1$ ), recombination current component ( $J_2$ ), shunt current component ( $J_{sh}$ ), and leakage current component ( $J_p$ ) by

this calculation method. Moreover, the modified 3-diode model was applicable at various cell temperatures.

Solely based on  $J$ – $V$  curve measurements and fitting by the modified 3-diode model, we can quantitatively analyze the electrical properties and output performance of Mc-Si solar cells with large leakage current through the periphery.

## References

- [1] S.K. Datta, K. Mukhopadhyay, S. Bandopadhyay, H. Saha, *Solid-State Electron* 35 (1992) 1667.
- [2] M. Chagaar, Z. Onennoughi, A. Hoffmann, *Solid-State Electron* 45 (2001) 293.
- [3] Z. Ouenoughi, M. Chagaar, *Solid-State Electron* 43 (1999) 1985.
- [4] K. Chakrabarty, S.N. Singh, *Solid-State Electron* 39 (1996) 577.
- [5] K. Kurobe, H. Matsumani, *Jpn. J. Appl. Phys.* 44 (2005) 8314.
- [6] K. Nishioka, N. Sakitani, K. Kurobe, Y. Yamamoto, Y. Ishikawa, Y. Uraoka, T. Fuyuki, *Jpn. J. Appl. Phys.* 42 (2003) 7175.
- [7] S.M. Sze, *Physics of Semiconductor Devices*, 2nd Ed, A Wiley-Interscience Publication, New York, 1981, p. 19.
- [8] K. Nishioka, T. Yagi, T. Hatayama, Y. Uraoka, T. Fuyuki, In: *Proc. 17th European Photovoltaic Solar Energy Conf.*, Munich, 2001, p. 1698.